Design and Implementation of Several Control Algorithms to an *in Silico* CSTR

Group 5

Spring 2017 Ch E 421 Final Project

May 5, 2017

Table of Contents

List of Tables and Figures

List of Abbreviations

FB	Feedback control algorithm
FF	Feedforward control algorithm
FFFB	Feedforward/Feedback control algorithm
FOPDT	First order plus dead time
P	Proportional control
PI	Proportional-Integral control
PID	Proportional-Integral-Derivative control algorithm
SOODPDTPL	Second-Order-Over-Damped-Plus-Dead-Time-Plus-Lead model
SP	Smith Predictor

List of Symbols

τ_I	Integral Time Constant
τ_D	Derivative Time Constant
τ_P^*	Process Time Constant
K_C	Proportional Gain (Controller Gain)
K_P^*	Process Gain
θ_P^*	Dead Time
G_P^*	Process transfer function
G_V	Valve transfer function
G_C	Controller transfer function
G_m	Measure transfer function
G_L^*	Load transfer function
T_J	Tank jacket temperature
T_M	Tank temperature

Introduction

For industries involving chemical reactions, it is often essential to keep reactors at a certain temperature. For this reason, reactors are equipped with temperature control systems. Process disturbances may occur in the inlet feed composition, inlet feed rate, and coolant inlet temperature. The goal of a process control strategy is to keep the tank temperature as close to the setpoint as possible during the process disturbances.

The objective of this project is to design three controllers and evaluate which strategy is most effective for controlling the tank temperature. Each control strategy is designed to provide improved control of the reactor temperature by manipulating the coolant flow rate through an equal percentage control valve. Figure 1 shows the piping and instrumentation diagram of the CSTR that was used for analysis in this report. The load disturbance variables for this process are feed flow rate, feed concentration, and the coolant inlet temperature. Also tested was the control systems response to a setpoint change. These disturbances were introduced sequentially at 100 second intervals throughout the process. A non–ideal proportional integral derivative (PID) control system, a second order plus dead time plus lead (SOPDPL) feedforward-feedback (FFFB) control system, and Smith Predictor are the control systems used to investigate the dynamics and control of the CSTR.

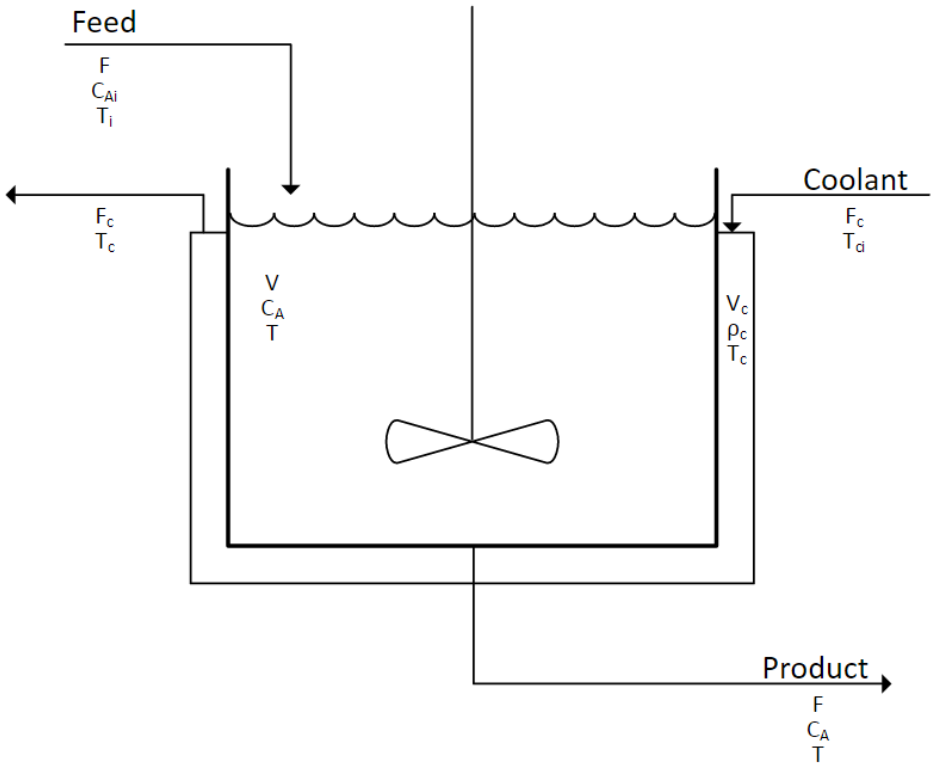

Figure 1. Piping and instrumentation diagram of a basic continuously-stirred tank reactor process analyzed in this project.

Theory, Assumptions, and Methodologies

Assumptions

To set the scope for analysis of the system, certain assumptions were made. All transmitters are assumed to be linear transmitters, just as all controllers are assumed to be reverse acting. The initial derivatives for all variables were assumed zero for all calculations—particularly for Euler's Method. Furthermore, it was assumed that no shaft work was performed by the system.

For the Second-Order-Over-Damped-Plus-Lead-Plus-Dead-Time transfer function, G_{ff}^{*} (refer to Equation 8) the exponential term is a negative time delay, which implies a predictive element. Because of that, the term is essentially removed or "punted out" of the equation as it makes the feedforward controller *physically unrealizable*. To be more specific, the controller is physically unrealizable because the numerator of the transfer function of the controller is a higher-order polynomial in s than the denominator. [1]

Proportional Integral Derivative control

Proportional, integral, and derivative controllers have a controller output based on a process parameter's deviation from setpoint, the integral over time of this error, and the derivative of this error, respectively. A proportional integral derivative controller (PID) is the combination of these three controller types, and removes some of the issues associated with them. A proportional only (P) controller will have an offset due to a setpoint change, as the controller output will change, reducing the error until it is constant, but not necessarily zero. This offset can be eliminated by adding the integral of the error to the control algorithm. Proportional control responds immediately to an error while integral control is slow, as the error must be present for a duration of time before the signal becomes significant. Another disadvantage of integral control is reset windup. After a sustained error, or large setpoint change, the integral term becomes large, and continues to increase until the measured parameter reaches its setpoint. This causes overshoot and oscillation.

Derivative control effectively anticipates large changes in the process. While the proportional and integral terms are not affected by how quickly the change happens, the derivative term will grow quite large for rapid changes. This is beneficial for certain scenarios, such as at the onset of a runaway reaction. Derivative control cannot be used alone, as the signal will be at the steady state value whenever the error is constant, no matter the value. Derivate and proportional controllers both have kick (undesirable, rapid, and large changes in signal). A proportional controller's signal will immediately change to a new value if an error is present. Rapid changes or fluctuations in the process will cause the derivative term to grow large. For this reason, they are not recommended for noisy processes. As seen in Equation 1, the ideal proportional derivative control is physically unrealizable due to a greater power of s in the numerator than the denominator of the transfer function. This results in an infinite signal in response to a step change; the derivative will be infinite after an instantaneous change. Thus the ideal PD controller is approximated by Equation 2 which is physically realizable and numerically similar.

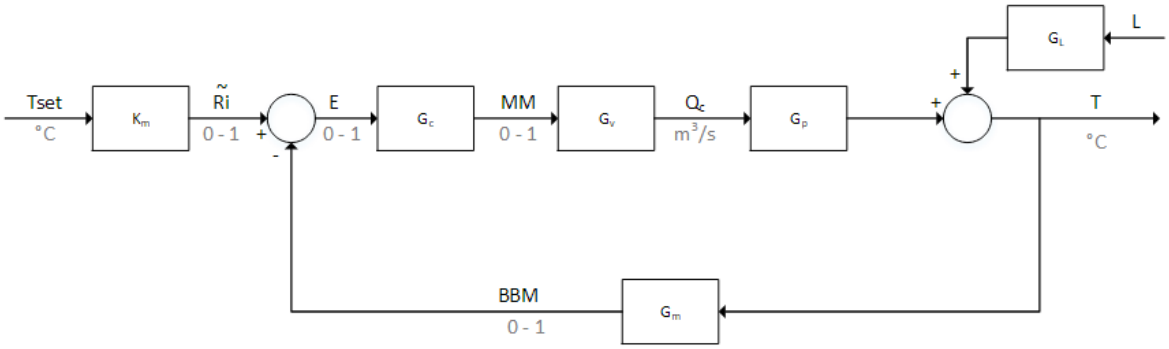

Figure 2: A PID Control model block diagram. All load variables, with their units, are shown for the FB Control model. Temperature (T) is the controlled variable, and flowrate (L) is the disturbance variable in the diagram.

Controller action

A controller can be reverse or direct acting. A direct acting controller will have an increase in its output signal due to an increased input signal, while a reverse acting controller will decrease its output in response to an increased input. Direct acting controllers therefore are characterized by a negative gain (K_c) and reverse acting controllers by a positive gain. Due to safety concerns or otherwise, a valve may be air to open or air to close. In order to have the correct response of the manipulated variable, given an air to open or air to close valve, a reverse or direct acting controller may be chosen. Once a valve type is chosen, the action of the controller can be selected to give the correct response of the manipulated variable.

Feedforward/Feedback Control

Feedforward-feedback (FFFB) control is a combination of feedback (FB) control, where corrections occur after the controlled variable deviates from a setpoint, and feedforward (FF) control, where disturbance variables are measured so preventative action can be taken. Feedforward control requires knowledge of how the disturbance and controlled variables respond to each other, so the accuracy of the control model is very important. Using feedforward and feedback control in combination alleviates this flaw in FF control, since the FB control will correct the control variable directly and track setpoint changes.

Problems with FB control arise when large or frequent disturbances occur, or the controlled variable cannot be measured on-line. Since FB control is responsive, rather than predictive, it is common to combine with feedforward control, which uses disturbance variables (rather than the controlled variable) as a basis for corrective action. The combination of feedback and feedforward control provides both predictive action to attempt to minimize process upsets, and responsive action after a disturbance has occurred.

In feedback control, no corrective action occurs until after a deviation in the control variable. It is a versatile and robust system that requires minimal knowledge about the process, because it acts based on deviations rather than predictions. Feedback control can be tuned to produce reliable control stand-alone; however, combined feedforward-feedback control demonstrates superior regulatory control to FBC alone, and therefore the two control systems are often used in conjunction.

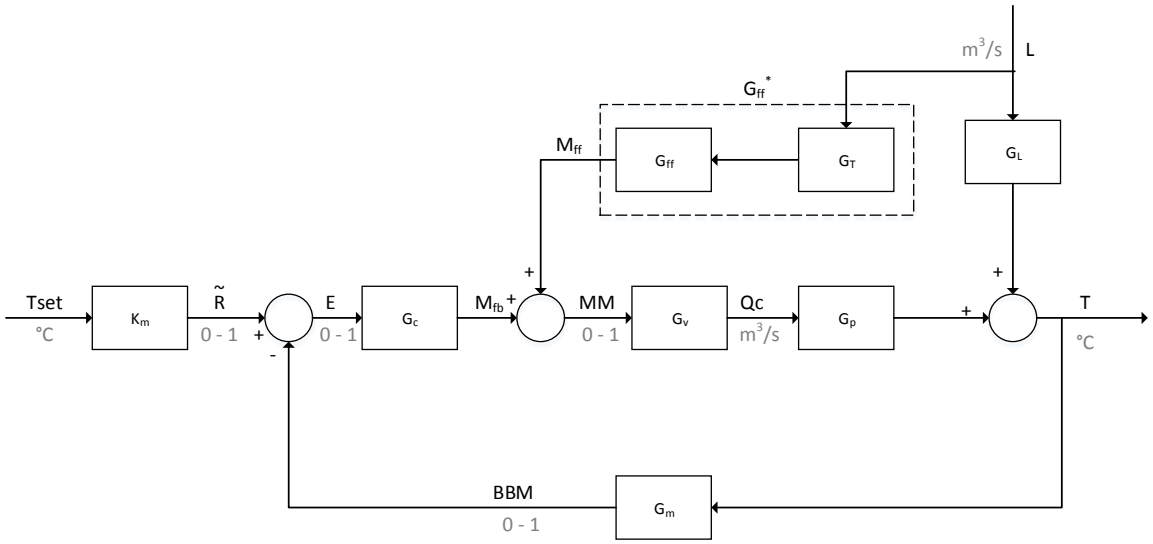

Figure 3: A Feedforward-Feedback Control model block diagram. All load variables, with their units, are shown for the FFFB Control model. Temperature (T) is the controlled variable, and flowrate (L) is the disturbance variable in the diagram

Table 1: FFFB block diagram in Figure 2 load variables and their units, along with a description.

Variable	Units	Value
T	°C	Controlled Variable (CV)
T^{SET}	°C	Set temperature
L	m^3/s	Load Variable
BBM	0-1	CV transmitter signal
$\tilde{R}$	0-1	Setpoint signal
E	0-1	Error
M_{fb}	0-1	Feedback signal
M_{ff}	0-1	Feedforward signal
MM	0-1	Combined FFFB signal
Q_c	m^3/s	Volumetric flow rate

Smith Predictor

The Smith Predictor is a control strategy that compensates for time-delays, effectively allowing for system control by predicting the system's state at a given time instant in the future. First developed by

O.J. Smith in the 1950's, the Smith Predictor includes a nested control loop to compensate for time delay, as seen with the $\widetilde{G_P}$ loop in Figure 3 [2]. The Smith Predictor control structure is a straightforward approach for time-delay control of Single Input Single Output (SISO) processes, and also may be extended to Multiple Input Multiple Output (MIMO) processes [3].

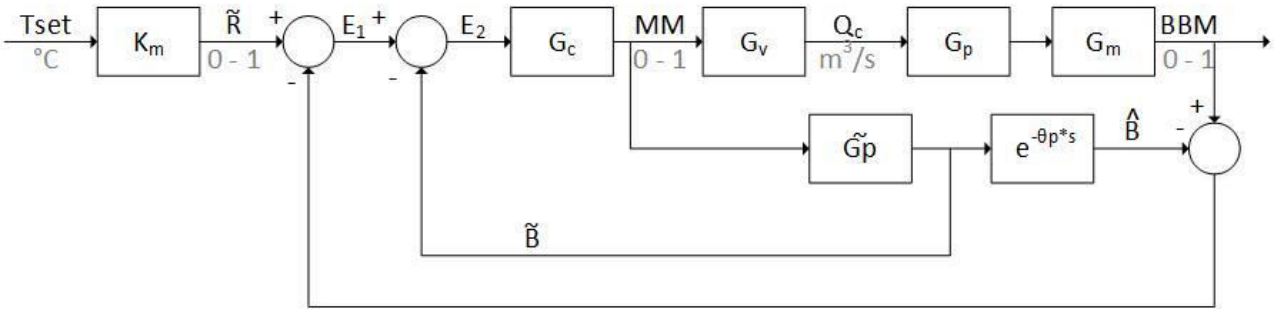

Figure 4. Block diagram for Smith Predictor control algorithm. Note the embedded control loop to compensate for time delay.

One of the best known time-delay compensation techniques, Smith Predictor effectiveness depends largely on the accuracy of the process model that corrects for time delay, $\widetilde{G_P}$. The time-delay process model is compared with the setpoint to arrive at E_1. Then, the Smith Predictor is accounted for by subtraction from E_1 to arrive at E_2. With an accurate model, a Smith Predictor can effectively compensate for time delays and reduce process deviation. However, an inaccurate process model leaves the Smith Predictor as an insufficient control strategy. This limits Smith Predictor flexibility and ability to adapt to large process changes [1].

The ability to predict the effect of process upsets is necessary for many industrial applications. For some systems, sensors must be placed far upstream from key control variables, which unfortunately creates a large dead time. Commonly, the dead time is attributed to the time it takes for the fluid to move through a pipe, but it can also be attributed to the time it takes for a given process to reach equilibrium. Using a Smith Predictor, one can decrease or even eliminate the negative effects of dead time upon process control.

More sophisticated processes require much more precise control than a standard FB or FBFF control for time-delay systems. For example, distillation columns often have very specific purification requirements. The products from distillation columns are usually sent through other processes, so a small upset in the column can have a huge impact on the plant as a whole. By adding a Smith Predictor to the feed stream, the compositions within the column can be maintained much more efficiently. Numerous high precision process apply the Smith Predictor strategy to remove variance without adding additional controllers.

Euler's Method

Euler's Method is a numerical method for approximating an ordinary differential equation, which is reformulated so it can be solved by arithmetic operations. An important concept in Euler's Method is local linearity, wherein multiple tangent line segments can be combined to approximate a curve. Euler's Method is a powerful and simple numerical method that only requires a few components: starting point,

step size, and the differential equation to be approximated. Even though the curve of a given differential equation is unknown, it can be approximated using the start point and differential equation to create a tangent line of the curve. Referencing local linearity, if the step size is small enough, the tangent lines can be combined to form an approximation of the differential equation's curve. [4] Thus at any time along the way, $New\ value = old\ value + slope \times step\ size$. [5].

¼ Decay Tuning Parameters

Accurate initial controller settings are vital to reduce the time required to tune controllers for optimal process control. Tuning controllers for an on-line process takes valuable time and introduces safety risks if the tuning is not executed properly. Quarter-decay tuning parameters are empirically derived tuning parameters for P only, proportional integral (PI), and PID control strategies in order to obtain closed-loop responses that have a quarter decay ratio for process response curves. Figure 5 illustrates the performance features of a step response of an underdamped process. Figure 5 also helps to explain the definition of decay ratio, which is just simply the ratio between the c- and a-magnitudes. A one-quarter decay ratio is then the ratio when $\frac{c}{a} = \frac{1}{4}$. First developed by Zeigler and Nichols in a 1942 publication, this methodology is also known as the Continuous Cycling Method, the Zeigler-Nichols method, and the Quarter Decay Ratio Response [6]. Specifically, proportional gain (Kc), integral time (τ_i), and derivative time (τ_D) are determined; specific equations are included in the Appendix.

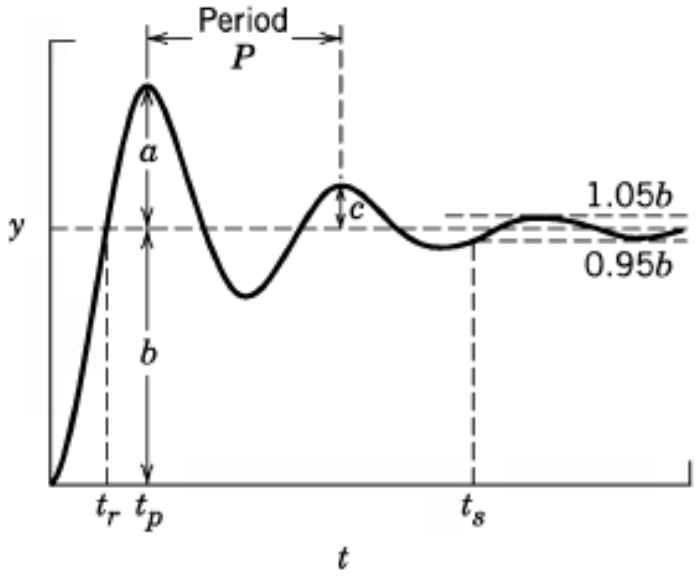

Figure 5: Performance features for a step response for a process with quarter decay tuning parameters [1].

Although this method is frequently recommended by control system vendors and used as a benchmark for evaluating different tuning methods, there are disadvantages. The experimental parameter development can be time consuming, process stability is likely at the limit of its stability, and the model does not apply for integrating processes, open-loop unstable processes, or first-order and second-order models without time delays [1]. In addition to the Quarter decay tuning parameters, there are other

strategies to arrive at initial tuning parameters, including the relay auto-tuning method, the step test method, and the Tyreus-Luyben method. [1]

Procedure

To start this process, a CSTR was taken to be operating in steady state. At time 0, the setpoint of the tank temperature was increased by 5°C. The system was given ample time to return to steady state, then three disturbances were introduced sequentially over 300 seconds. At the 400 second mark, all of the process variables are returned to their initial values.

The first disturbance to be applied was a 20% increase in the feed flow rate. As show in Figure 4, the feed was initially at 0.45 m^3/s, then at 100 seconds it was raised to 0.54 m^3/s. Finally at 400 seconds, the flow rate was set back to its starting value of 0.45 m^3/s.

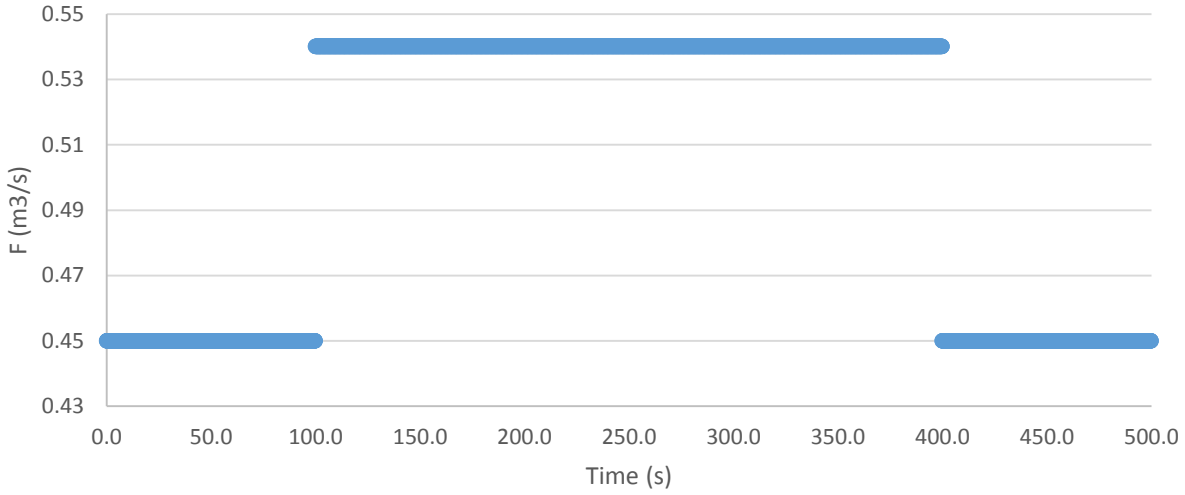

Figure 6: Process step change showing the changes in the CSTR feed rate over 500 seconds. A step change of +20% occurs at 100 seconds, and another step change of -20% occurs at 400 seconds.

The second disturbance to be examined was an upset in the feed concentration. Figure 5 shows the concentration being decreased by 5% between 200 and 400 seconds. The concentration of component A started at 2.88 $kgmol/m^3$ and was dropped to 2.74 $kgmol/m^3$, before being returned to its initial value at 400 seconds.

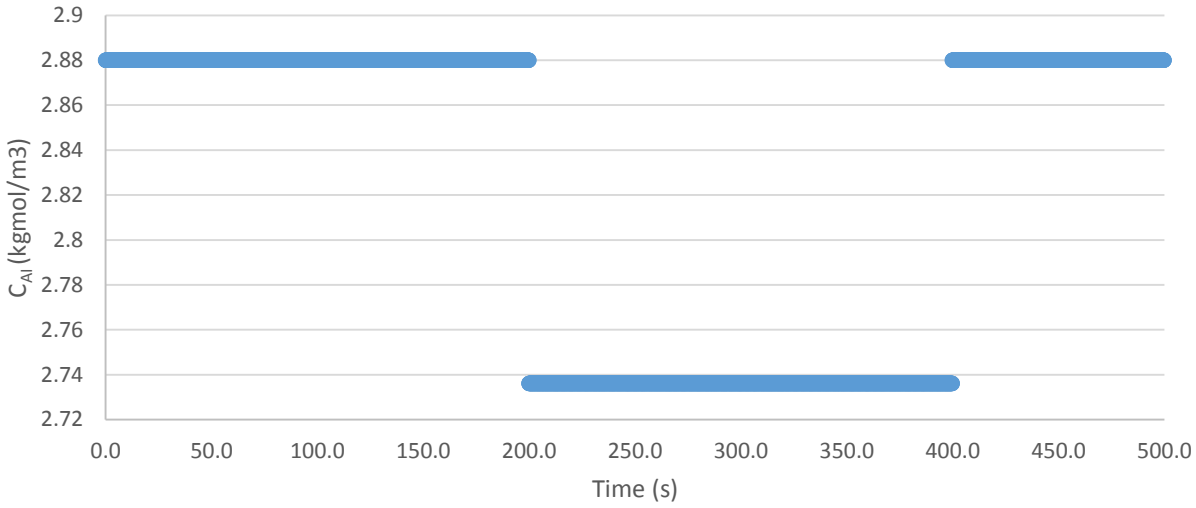

Figure 7: Process step change showing changes in the concentration of species A in the feed stream of the CSTR. Composition load disturbances of -5% and +5% occur at 200 and 400 seconds respectively.

The final disturbance to be tested was a change in the coolant inlet temperature. At 300 seconds, the coolant temperature was increased by 5°C. Once again, the value was returned to its initial setpoint at 400 seconds. This change in temperature can be seen graphically in Figure 6.

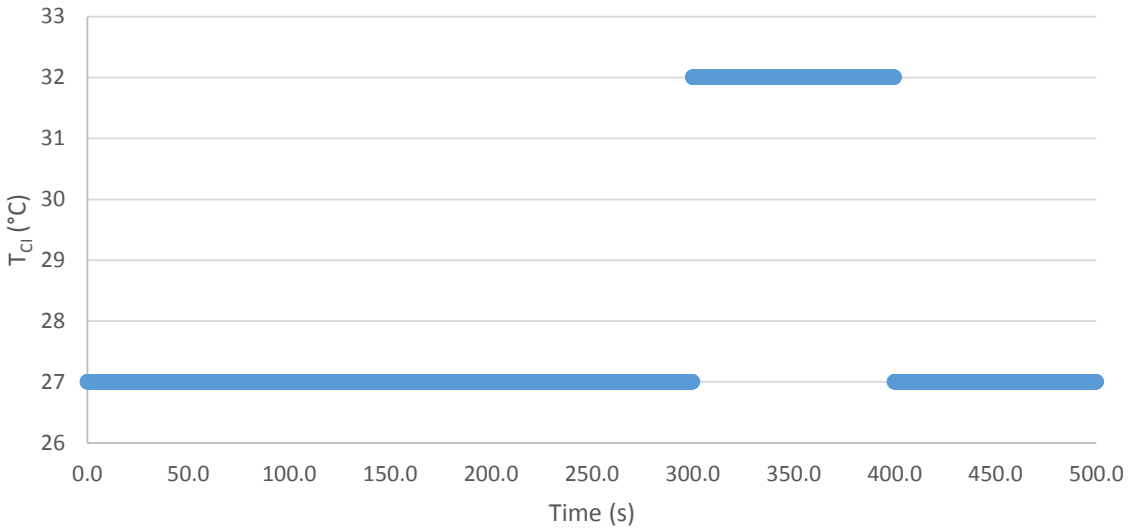

Figure 8: Process step change showing the coolant inlet temperature change over 500 seconds. Disturbances to the coolant inlet temperature of +5% and -5% occur at 300 and 400 seconds respectively.

Discussion of Results

Non-Ideal PID Controller

The selected tuning parameters have a significant impact on the quality of the controller. If the values of τ_D or τ_I were too high, the response of the controller was slow, though too small of values resulted in overshoot and occasional oscillation in response to a disturbance or setpoint change. K_c showed an opposite response; too low a value resulted in a slow response, and too high a value caused overshoot. If too high or low a value of α was chosen, an erratic or oscillatory response was observed. The parameters shown in Table 3 returned the process to its setpoint as quickly as possible without significant overshoot.

Parameters for G_P^* were found by fitting a first order plus dead time (FOPDT) model to process data, using Excel Solver to minimize the sum of squared error. This result is shown in Figure 9. The tuning parameters obtained while determining the process reaction curve are shown in Table 2 and Table 3.

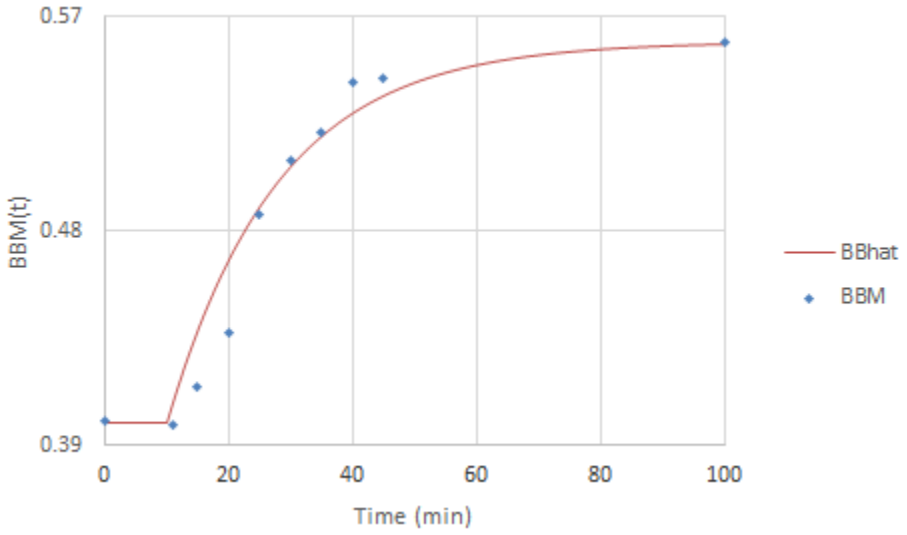

Figure 9. Process Reaction Curve for a First Order System

Table 2. G_P^* parameters determined by fitting a FOPDT model to system data, as shown in Figure 7.

	Gp*
K_p^*	1.71
θ_p^*	10.00
τ_p^*	19.14

Table 3. Recommended tuning parameters for feedback PID controller

	Initial	Final
Kc	0.35	0.40
τ_I	20.00	15.00
τ_D	5.00	3.00
α	0.10	0.09

Figure 10 shows that the tank temperature changed quickly in response to a setpoint change, yet did not overshoot. All of the disturbances that occurred resulted in an initial deviation from setpoint, but were corrected well by the controller.

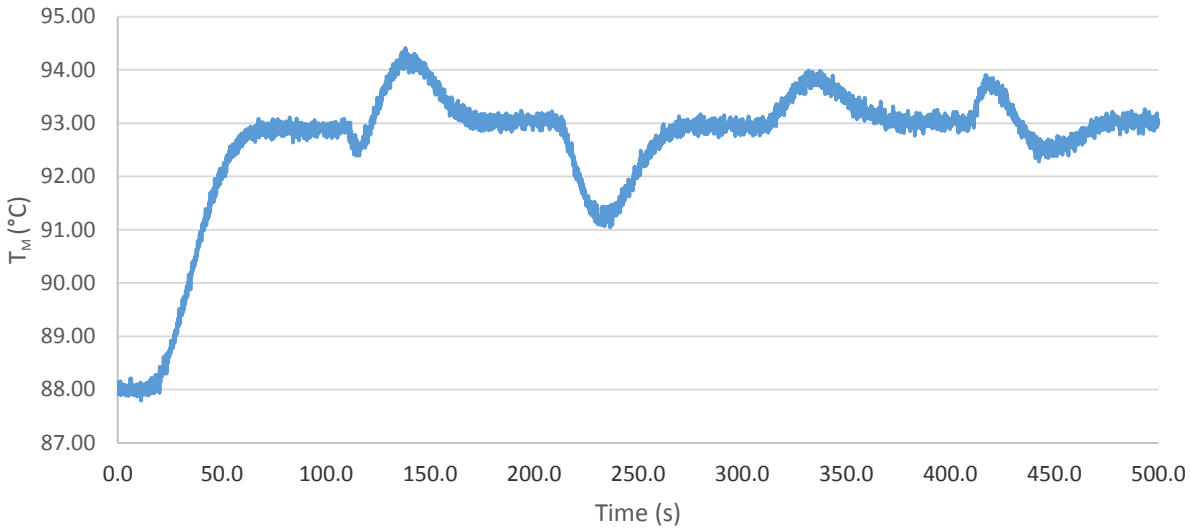

Figure 10: CSTR tank temperature (T_M) in response to change in process parameters using feedback PID control

The disturbances to the system resulted in changes to the coolant outlet temperature. As expected, when the tank operated at a higher temperature, the coolant exit temperature was also higher, as shown in Figure 11.

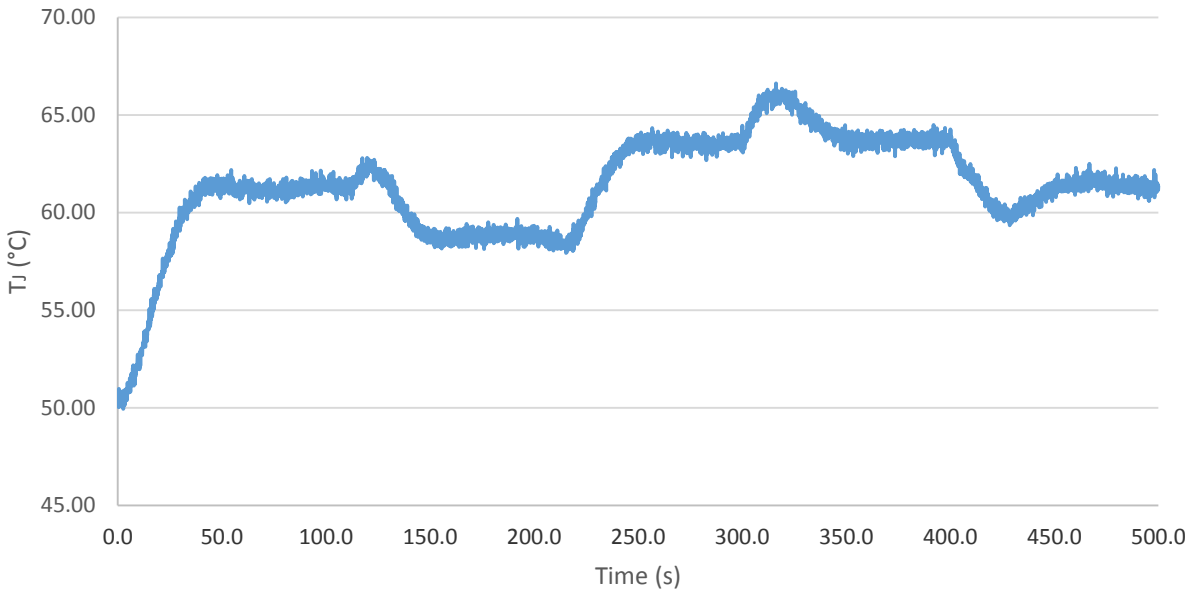

Figure 11. CSTR jacket temperature (T_J) in response to the change in process parameters using feedback PID control

The temperature transmitter signal is proportional to temperature. This is because the transmitter is linear, therefore similarities in action can be seen between Figure 10 and Figure 12.

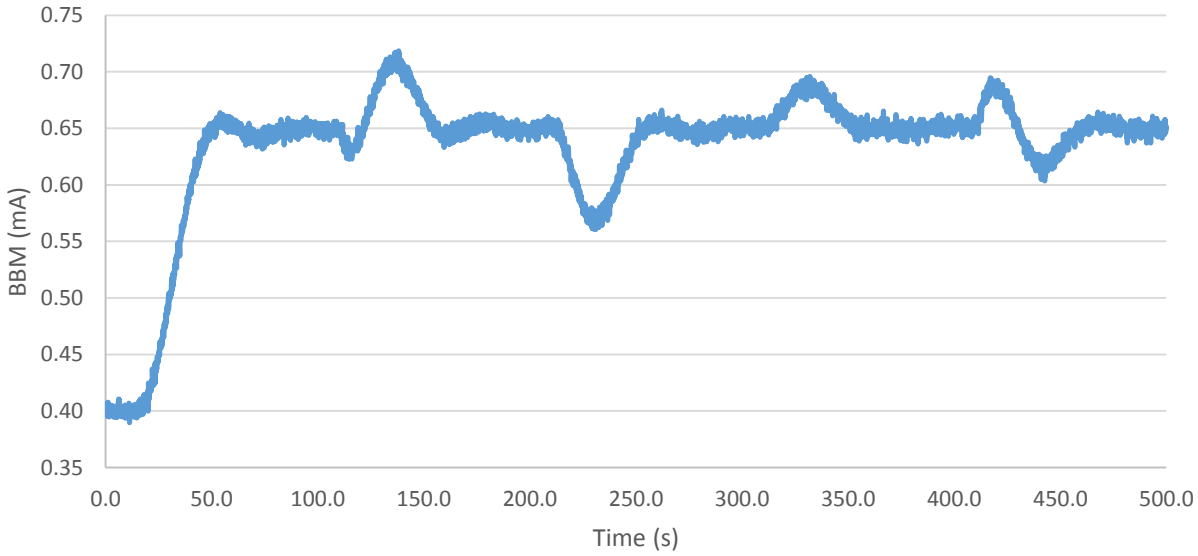

Figure 12: Process reaction curve for temperature transmitter signal.

Figure 13 shows the coolant flow rate response through an equal percentage valve. The plot shows the effect the load disturbances–feed rate, feed composition, and coolant inlet temperature—have on the coolant flow rate. A step change of $+5$ ℃ in the set point of the reactor temperature reached a new set point of 93℃ 72 seconds after the step change was first introduced. This step change produced the

response shown in Figure 13 between 0 and 100 s. Because of this step change, a decrease in the coolant flow rate was observed. In order to reach a higher jacket temperature and thus a higher reactor temperature, less heat was absorbed by the coolant flow rate entering the system.

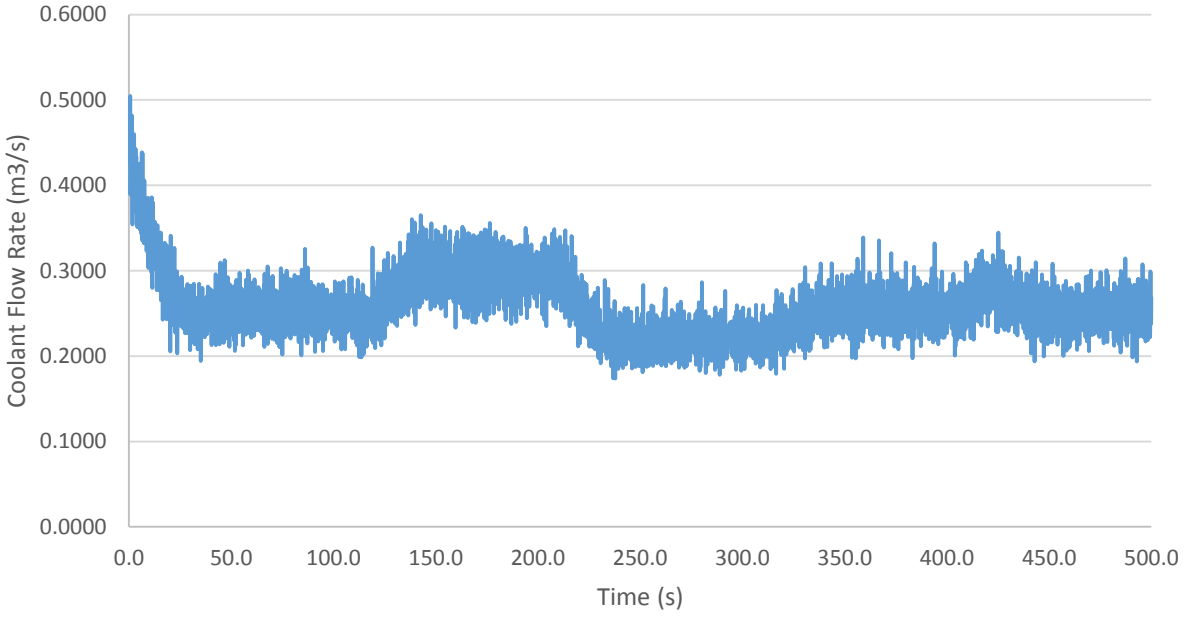

Figure 13: Coolant flow rate response through equal percent valve.

After the setpoint is altered, the coolant flowrate through the equal percentage valve reaches a new steady state in approximately 25 seconds. After 100 seconds, the $+20\%$ feed rate load disturbance caused an increase in the coolant flow rate. This demonstrated that as more heat was generated because of exothermic chemical reaction and a higher temperature of the reactor was reached, a greater coolant flow rate must be used to decrease the jacket temperature and thus the reactor temperature. After 200 seconds, a -5% feed composition change was imposed. Consequently, heat production and reactor temperature decreased. To overcome this change, the coolant flow rate was decreased as a response to that change. After 300 seconds, a coolant inlet temperature change of $+5℃$ was imposed. This resulted in an increase of the reactor and jacket temperatures. A small coolant flowrate temperature response can be appreciated in Figure 13 as consequence of the coolant inlet temperature load disturbance. After 400 seconds, a feed rate change of -20%, a feed composition change of $+5\%$, and a coolant temperature disturbance of $-5℃$ were imposed. The coolant flow rate response shown in Figure 13 was recorded. As with the previously mentioned load disturbances, a decrease in feed rate produced a decreased coolant flow rate; increased composition load caused an increased coolant flow rate; finally, decreased coolant temperature triggered decreased coolant flow rate.

Feedforward/Feedback Control (FFFB)

The Feedforward-Feedback Control (FFFBC) model was also explored in this project. Combining Feedforward Control with Feedback Control allows for predictive corrective action by measuring a disturbance variable through Feedforward Control. The disturbance variable that is measured is the inlet feed rate, as shown below in Figure 14. The Feedforward portion of the block diagram is demonstrated with the addition of a Flow Transmitter to the Feed line, which connects directly to the Temperature Controller. When integrated with the existing feedback controller, FFFB allows for a better control of a chemical process by enabling predictive and responsive action.

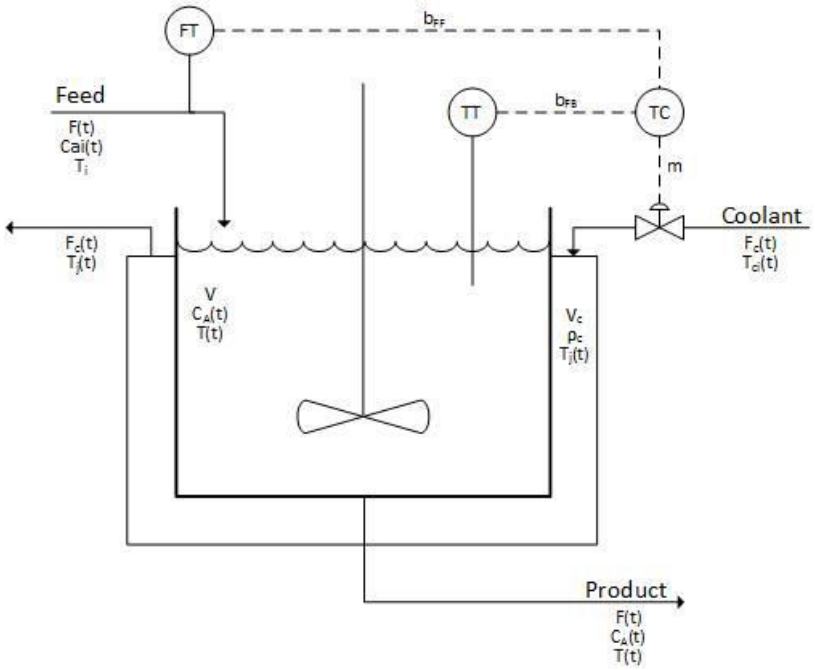

Figure 14: Piping & Instrumentation Diagram for the modeled FFFB Control system on a CSTR.

An equation of the FFFB Control model is represented by the following equation:

$$\frac{M_{ff}^{'}(s)}{F^{'}(s)} = -\frac{k_L^*(\tau_{La}^*s+1)(\tau_P^*s+1)}{k_P^*(\tau_{L1}^*s+1)(\tau_{L2}^*s+1)} e^{-(\theta_L^*-\theta_P^*)s} \quad \frac{M_{ff}^{'}(s)}{F^{'}(s)} = -\frac{k_L^*(\tau_{La}^*s+1)(\tau_P^*s+1)}{k_P^*(\tau_{L1}^*s+1)(\tau_{L2}^*s+1)} e^{-(\theta_L^*-\theta_P^*)s} \qquad \text{Equation 8}$$

A detailed derivation can be found in the report Appendix. Using Euler's and ¼ Decay Methodologies, the tuning parameters shown in Table 4 were calculated.

A Second-Order-Over-Damped-Plus-Dead-Time-Plus-Lead (SOODPDTPL) was implemented to create a Feedback/Feedforward controller for the CSTR process. This model was determined using Euler's method for a 20% step change in the feed flow rate at time 100 sec. Parameters of G_L^* in Table 4 were

solved for using a fit to a second order over-damped plus dead time plus lead (SOODPDTPL) system seen in Figure 15 and solver. Values from G_P^* in Table 2 that were discussed in the PID Controller section were also used in the FFFBC equation.

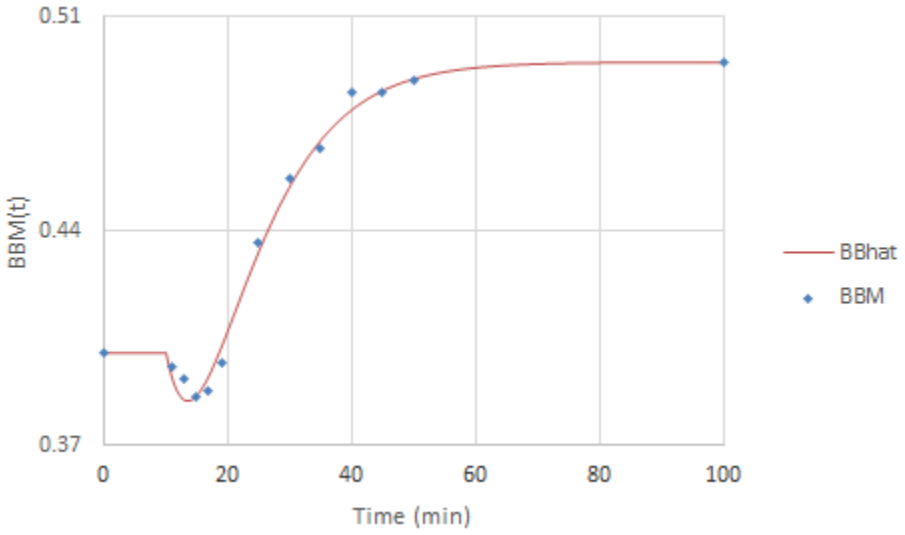

Figure 15: Second-Order-Over-Damped-Plus-Dead-Time-Plus-Lead process reaction curve.

Table 4: G_l^* parameters were calculated using a SOODPDTPL system and nonlinear regression.

$\boldsymbol{G_L^*}$	
K_L^*	1.055556
θ_L^*	10 s
τ_{La}^*	-6.20709 s
τ_{L1}^*	7.756908 s
τ_{L2}^*	7.756917 s

As discussed in the Feedback Controller, tuning parameters have significant impact on controller quality. Final tuning parameters for Kc, τ_I, τ_D, and α were found by decreasing the parameters' initial values in

Table 5 until the FFFB graphical response had minimal oscillations and quickly reached new setpoints. The final parameters calculated result in a controller that reaches the new tank temperature quickly, while minimizing oscillations and overshoot. Decreasing K_c, τ_D, and τ_I produced an output with reduced oscillations. Decreasing K_C beyond our final value did not produce desired output – it gave the output a positive slope, and did not return to setpoint values. Decreasing τ_D and τ_I beyond our final value created additional overshoot.

Since the tuning parameters for FFFBC were derived from the PID controller, tuning the FFFB Controller yielded similar results of minimizing oscillations and overshoot levels when changing K_C, τ_D and τ_I.

Table 5: Recommended and tuned parameters for the FFFB Controller.

	Initial	Final
K_C	1.34	0.40
τ_I	20.00 s	15.00 s
τ_D	5.00 s	3.00 s
α	0.10 s	0.04 s

Figure 16 shown below is a graphical output of temperature in the CSTR for a FBFF PID control system over 500 seconds. The temperature in the tank is seen to fluctuate after the disturbance was created.

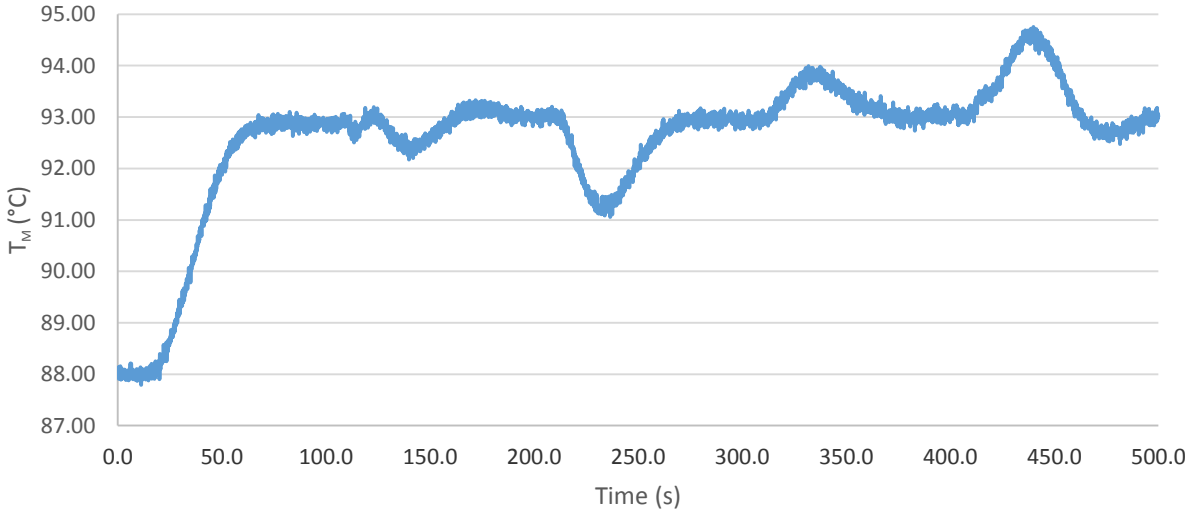

Figure 16: Graphical output for the Feedback-Feedforward Control response. Over a time of 500 seconds, process variables such as temperature setpoint, feed rate load disturbance, coolant inlet temperature load, and feed composition load were changed. This graphical output shows the response of the FFFB Control System to these changes.

Figure 17 is the graphical output of the CSTR jacket temperature over time. The effect of changes in temperature, feed concentration, and feed rate were also seen on the CSTR jacket temperature output. The responses of the tank temperature and the CSTR jacket temperature are very similar, as they reach steady states at similar times. For example, at a time of 300 seconds, the jacket temperature responds to the +5% change in the coolant temperature, but returns back to its original steady state. This is because the controller responded by increasing the coolant's flow rate, to allow the tank temperature to once again achieve its setpoint of 93°C.

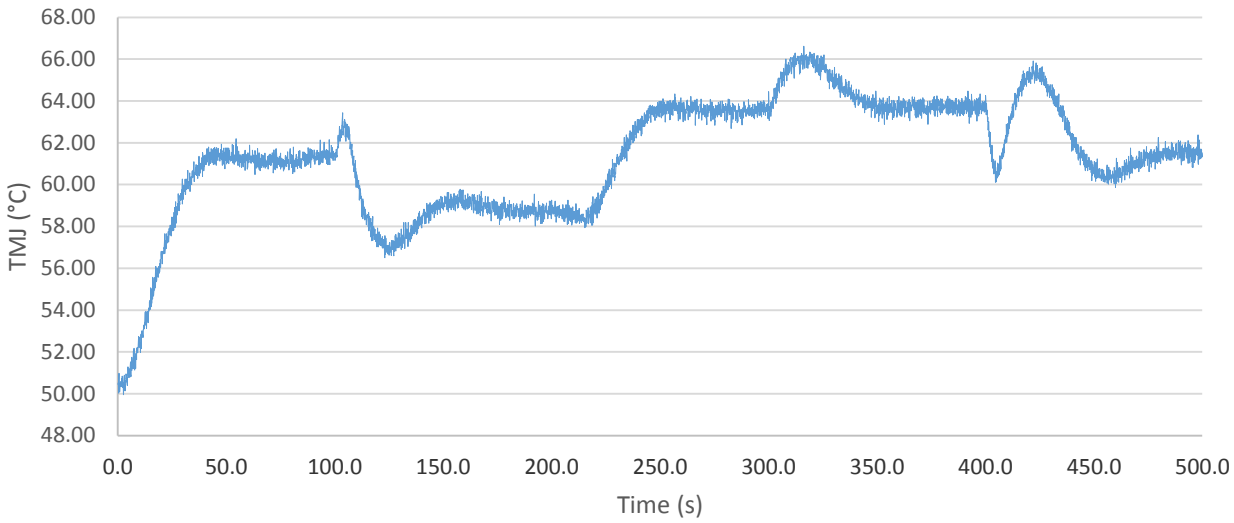

Figure 17: CSTR jacket temperature plotted against time for the FFFBC model.

Smith Predictor

The Smith Predictor is a control strategy developed to compensate for time delays. The controller receives input from a transmitter upstream of the controlled variable and uses a dynamic process model to make adjustments in order to dampen control variable deviation.

The CSTR system utilized a flow transmitter on the tank feed stream to inform the tank temperature controller of upsets in the feed flow before tank temperature deviations were measured. This type of model allows for the controller to dampen system deviations and return the process to setpoint quicker than other strategies. A complete piping and instrumentation diagram of the Smith Predictor system is displayed in Figure 18 below.

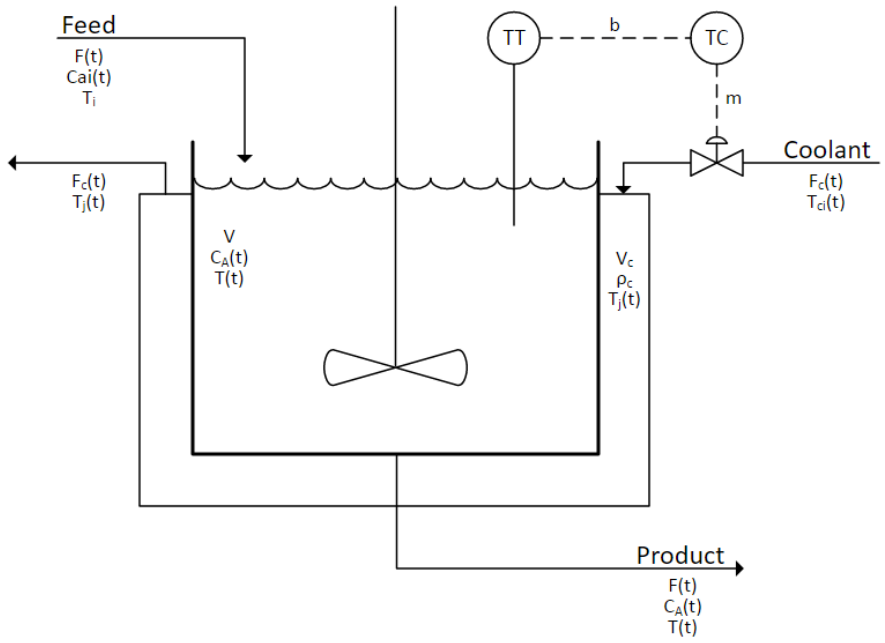

Figure 18. Piping and instrumentation diagram of the system, properly equipped with the necessary transmitters to use Smith Predictor control.

Smith Predictor control uses a process model to interpret process inputs to control action. For this control strategy, multiple transfer functions were utilized and three of those transfer functions were combined to create the overall transfer function G_p* seen in Equation 13. The full derivation of the Smith Predictor can be found in the Smith Predictor Derivation section of the Appendix.

$$G_P^* = \frac{\hat{B}(s)}{MM(s)} = \frac{k_P^* e^{-(\theta_P^* s)}}{\tau_P^* s + 1} \qquad \text{Equation 13}$$

The process model used for the Smith Predictor was developed in the PID feedback controller, derived in the Smith Predictor Derivation section of the appendix. Initial tuning parameters were taken from the Feedback controller. The Smith Predictor was further tuned to optimize the response time for tank temperature (TM) without overshoot. The Tank temperature over the period of time observed (500 s) is displayed in Figure 19 below.

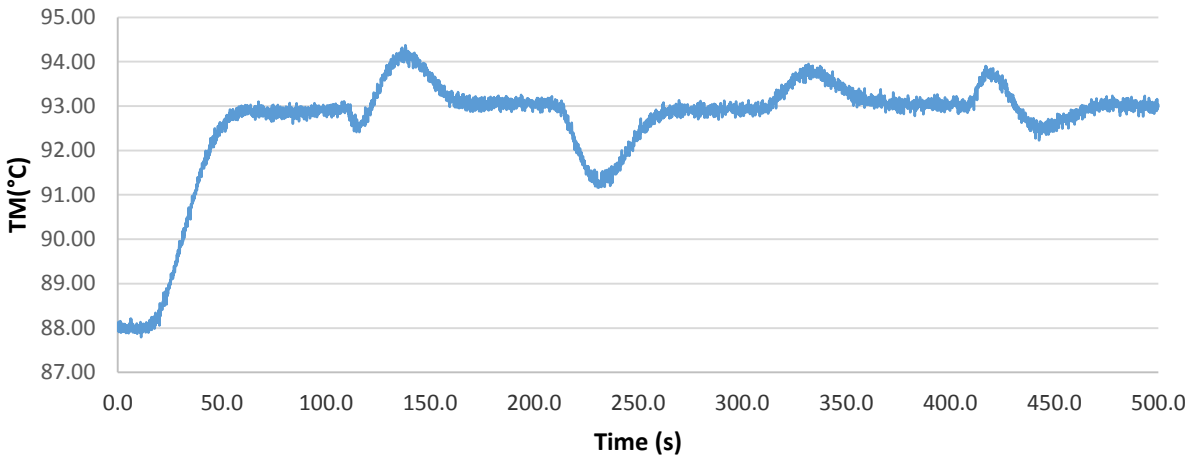

Figure 19: The tank temperature measured over the observed time, 500 s, when controlled by the Smith Predictor.

The overall objective was to reach the setpoint as quickly as possible without overshoot. The key to achieving the best result was maximizing the gain, Kc. Greater gain results in a more responsive process, but also a process more prone to overcorrection. This is consistent with discussion in class and from the text from Seborg et. al. The gain was gradually increased and the other parameters were manipulated to remove overshoot. Increasing τ_i and τ_d can slow the response time and eliminate overshoot. Because the response showed a slightly higher dependence on τ_i, it was adjusted first and τ_d was just used for fine tuning. Increasing α marginally increased the response time, but also created oscillation; thus α was held at 0.1.

The final tuned parameters were on the same order as the initial tuning parameters, indicating quality initial tuning parameters. Initial tuning parameters were developed from the Ziegler-Nichols Quarter Decay Response Ratio, detailed specifically in Table 6 in the Appendix. Initial tuning parameters are important in order to minimize the tuning required for a particular controller.

The temperature within the jacket of the CSTR varied in response to the process disturbances, as discussed earlier. As displayed in Figure 20, the average temperature in the jacket increases when the tank temperature was increased by 5°C at time 0. A small amount of overshoot occurred after each disturbance was applied. This overshoot gives some explanation of how the Smith Predictor is able to reach steady state faster than a feedback system. By overcorrecting beyond the steady state value, there is an increased temperature difference between the tank jacket and the tank contents, creating a larger driving force for temperature change that leads to a quicker tank temperature response.

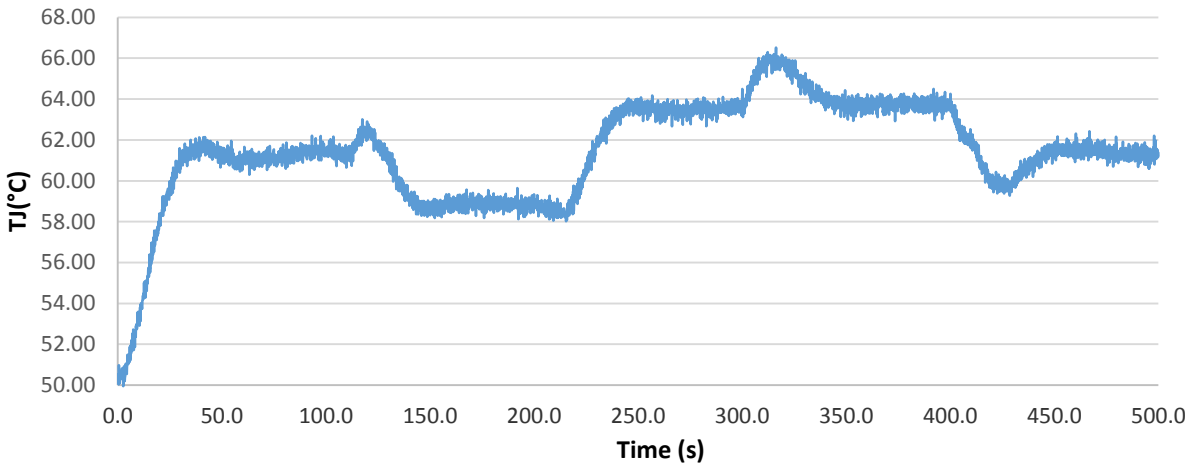

Figure 20. The tank jacket temperature measured over the observed time, 500 s, for a Smith Predictor-controlled system.

Comparisons

The three control systems used performed similarly for most disturbances, as shown in Figure 21, though the FBFF controller could more readily handle changes in flow rate, such as at times of 100 and 400 seconds. This is expected since the FBFF controller has an extra sensor on the feed to anticipate the temperature change based on a flow rate change. For all other disturbances, the Smith Predictor responds the most quickly with less of a disturbance. This advantage, however, is rather small.

A potential downside of the FBFF system is that it has a significant amount of oscillation in response to flow rate changes. This could likely be corrected by adjusting the tuning parameters, specifically those associated with the FF part of the equation. In this experiment, the FBFF parameters were left equal to the FF parameters for comparison.

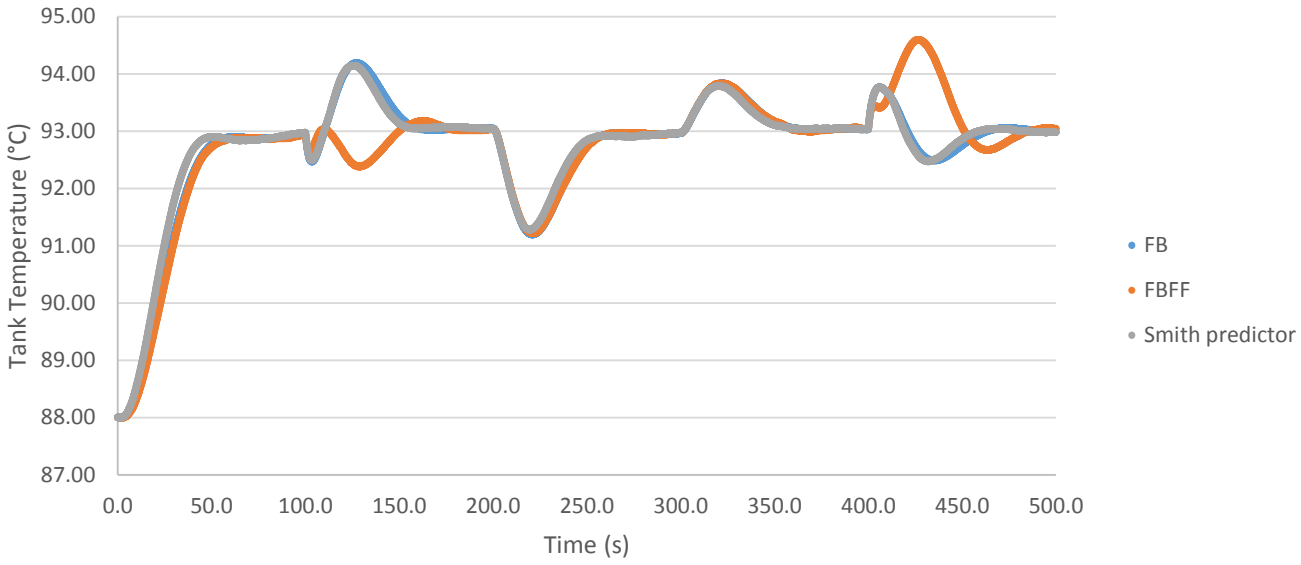

Figure 21: Tank temperature in response to disturbances for different control strategies

The coolant flowrates, seen Figure 22, are very similar for all control algorithms except for the FBFF method in response to a flowrate change. As seen at 100 and 400 seconds, the coolant flow rate changed very dramatically when the feed flow rate was adjusted. It should be noted that for all of the other process changes the SP controller adjusted the coolant flow rate slightly quicker than the other two controllers.

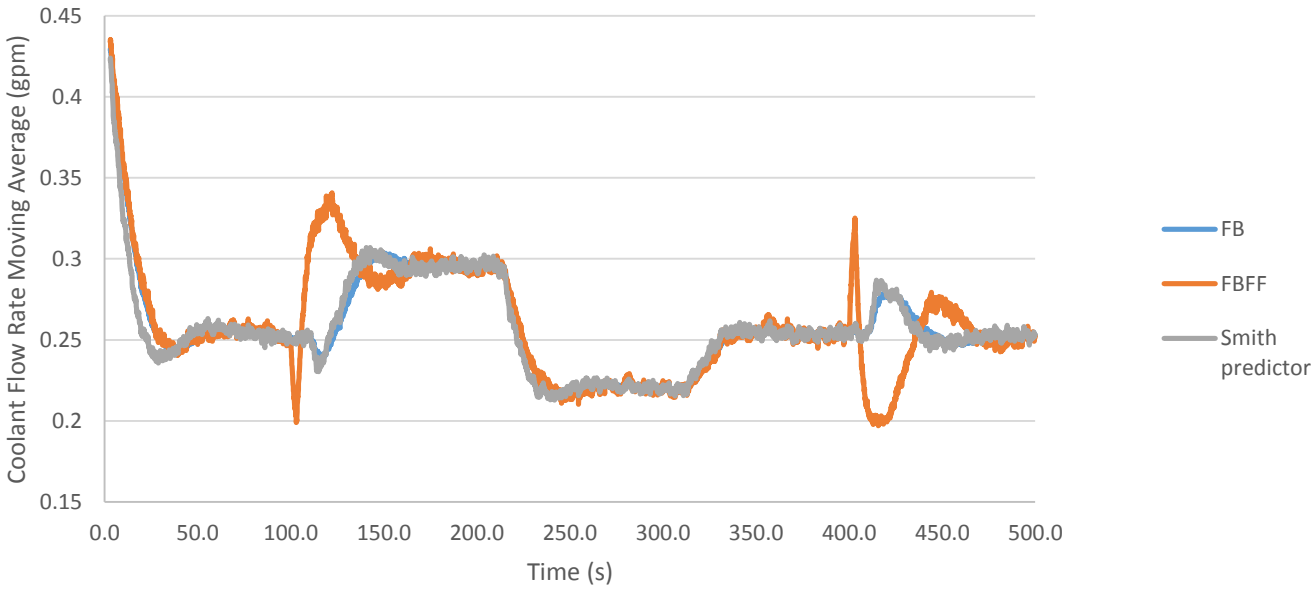

Figure 22: 30 period moving average of coolant flowrate in response to process changes

Conclusions

Several different control algorithms were implemented for process control of an *in Silico* CSTR. A non-ideal PID feedback controller was initially developed. Then, a feedforward loop was added to this feedback control to construct feedforward-feedback control. Finally, the Smith Predictor technique was applied to the feedback controller in order to compensate for time delay. Each model used transfer functions to model process responses for given inputs and load disturbances.

Each controller has unique application that is best suited for specific scenarios. Overall, all three strategies controlled the process very similarly, reflecting the identical nature of the FB algorithm in each of the controllers. The SP produced the fastest result to the process setpoint change at time zero, demonstrating the advantage of time compensation. FFFB control responded differently to process disturbances that involved the inlet feed rate at t=100 s and t=400 s that was being controlled by FF control. Thus, the controller reacted in a manner opposite to the SP and FB controllers, indicating the power of upstream measurement and feedforward control. However, the overall time for the process to return to setpoint was not significantly different among any of the controllers.

It is not a simple decision selecting what type of controller is best for a given process; however, certain generalizations have been demonstrated by this CSTR process. Feedback control is required for almost any controller in order to compare the measured variable to the setpoint value and react to the error. FF control can be beneficial in responding more quickly to certain process deviations ahead of error in the setpoint; however, experimentation is necessary to determine if this more precise control yields a

higher performance control system. For systems with significant time-delay, an approach that utilizes time-compensation can be very valuable. The Smith Predictor is one of the most popular techniques and was used successfully for this CSTR system.

For any controlled process, it is paramount to understand the algorithms behind the controllers and to analyze how process disturbances affect the setpoint. It is not enough for engineers to assume initial tuning parameters will be sufficient, or that one control strategy will work for different processes. Careful development of and experimentation with a process model control strategy is important to build understanding. Eventually, live testing and pilot scale may be needed in order to confidently approach the implementation of control processes and on-line tuning required. Whatever process an engineer approaches, proper control will help maximize efficiency and optimize production for a robust process, all while maintaining excellent safety.

The error involved in the measurements and calculations for the CSTR system must be understood for complete analysis. Although process measurements are intended to be accurate, there is always imperfect mixing, equipment material, and instrument error that obstruct that accuracy. For diagnostics such as process temperature, a vessel measurement will only measure the temperature of the process fluid for that specific area. A lack of mixing or the specific heat of process equipment may introduce error into that measurement reading. Specific measurement error can be identified from the specific instrument performing the measurement and an in-depth study of the process dynamics. All measurement error should be propagated appropriately through calculations.

Recommendations

Looking forward to future research, there are many opportunities to further students understanding. Because the tuning parameters are adjusted using a guess and check method, it might be helpful to develop a dynamic model to show the effect of changing tuning parameters. For example, one could create a macro in Excel that would allow you to quickly change the tuning parameters without having to type in new values every time. Being able to make quick changes is vital because it can be difficult to hone in on the optimal values for each parameter.

Another potential area to research would be different types of controllers. Ratio control could be examined as an alternate form of feedforward control. Ratio control is typically used to maintain stoichiometric ratios, but it can also be used to manipulate other variables. Additionally, a cascade control system could be tested. Cascade controls are often used to improve the response to a setpoint change by utilizing intermediate measurement point and two feedback controllers [1]. A recommendation would be for the future classes to analyze a cascade control system for controlling this process. These types of controllers are very widely used in industry and would be beneficial for students to be familiar with.

References

[1] D. E. Seborg, T. F. Edgar, D. A. Mellichamp and F. J. Doyle III, Process Dyanmics and Control, 3rd ed., Hoboken, NJ: John Wiley & Sons, Inc., 2011.

[2] S. R. K. Veeramachaneni, "Robust pid control using a smith predictor for time delay systems," Wichita State University, Wichita, 2013.

[3] P. Sourdille and A. O'Dwyer, "A new modified smith predictor design," in *Dublin Institute of Technology Arrow@DIT*, Dublin, 2003.

[4] K. A. Atkinson, An Introduction to Numerical Analysis, New York: John Wiley & Sons, 1989.

[5] S. C. Chapra, Applied Numerical Methods with MATLAB, New York: The McGraw-Hill Companies, Inc., 2012.

[6] L. C. Faculty, "Continuous Cycling," 10 February 2016. [Online]. Available: https://www.youtube.com/watch?v=dEUGAH4JOdI. [Accessed 30 April 2017].

Appendix

PID Derivation

$$\frac{MM'(s)}{E'(s)} = K_c\left(\frac{\tau_I s+1}{\tau_I s}\right)\left(\frac{\tau_D s+1}{\alpha\tau_D s+1}\right) \qquad \textit{Equation 1}$$

$$(\alpha\tau_I\tau_D s^2 + \tau_I s)MM'(s) = K_c[\tau_I\tau_D s^2 + (\tau_D + \tau_I)s + 1]E'(s) \qquad \textit{Equation 2}$$

$$\alpha\tau_I\tau_D\frac{d^2MM'(t)}{dt^2} + \tau_I\frac{dMM'(t)}{dt} = K_c(\tau_I\tau_D\frac{d^2E'(t)}{dt^2} + (\tau_D + \tau_I)\frac{dE'(t)}{dt} + E'(t)) \qquad \textit{Equation 3}$$

$$\frac{d^2MM'(t)}{dt^2} = \frac{K_c(\tau_I\tau_D\frac{d^2E'(t)}{dt^2}+(\tau_D+\tau_I)\frac{dE'(t)}{dt}+E'(t))-\tau_I\frac{dMM'(t)}{dt}}{\alpha\tau_I\tau_D} \qquad \textit{Equation 4}$$

Feedforward-Feedback Derivation

$$\frac{BBM}{F} = \frac{(-G_L+G_TG_{ff}G_VG_P)G_M}{1+G_CG_VG_PG_M} \qquad \textit{Equation 5}$$

$$G_{ff}^* = \frac{M'_{ff}(s)}{F'(s)} = -\frac{G_L^*}{G_P^*} \qquad \textit{Equation 6}$$

$$G_{ff}^* = \frac{\frac{k_L^*(\tau_{La}^*s+1)e^{-\theta_L^*s}}{-(\tau_{L1}^*s+1)(\tau_{L2}^*s+1)}}{\frac{k_P^*e^{-\theta_P^*s}}{\tau_P^*s+1}} \qquad \textit{Equation 7}$$

$$\frac{M'_{ff}(s)}{F'(s)} = -\frac{k_L^*(\tau_{La}^*s+1)(\tau_P^*s+1)}{k_P^*(\tau_{L1}^*s+1)(\tau_{L2}^*s+1)}e^{-(\theta_L^*-\theta_P^*)s}\frac{M'_{ff}(s)}{F'(s)} = -\frac{k_L^*(\tau_{La}^*s+1)(\tau_P^*s+1)}{k_P^*(\tau_{L1}^*s+1)(\tau_{L2}^*s+1)}e^{-(\theta_L^*-\theta_P^*)s} \qquad \textit{Equation 8}$$

After the cancellation of the exponential expression in the equation shown above, the following equation is obtained

$$\frac{M'_{ff}(s)}{F'(s)} = -\frac{k_L^*(\tau_{La}^* s+1)(\tau_P^* s+1)}{k_P^*(\tau_{L1}^* s+1)(\tau_{L2}^* s+1)} \quad \textit{Equation 9}$$

$$[\tau_{L1}^*\tau_{L2}^* s^2 + (\tau_{L1}^* + \tau_{L2}^*)s + 1]M'_{ff} = -\frac{k_L^*}{k_P^*}[\tau_{La}^*\tau_P^* s^2 + (\tau_{La}^* + \tau_P^*)s + 1]F'(s) \quad \textit{Equation 10}$$

$$\tau_{L1}^*\tau_{L2}^*\frac{d^2M'_{ff}}{dt^2} + (\tau_{L1}^* + \tau_{L2}^*)\frac{dM'_{ff}}{dt} + M'_{ff} = -\frac{k_L^*}{k_P^*}(\tau_{La}^*\tau_P^*\frac{d^2F'(t)}{d^2t} + (\tau_{La}^* + \tau_P^*)\frac{dF'(t)}{dt} + F'(t) \quad \textit{Equation 11}$$

$$\frac{d^2M'_{ff}}{dt^2} = -\frac{k_L^*}{k_P^*}\frac{\left(\tau_{La}^*\tau_P^*\frac{d^2F'(t)}{dt^2}(\tau_{La}^*+\tau_P^*)\frac{dF'(t)}{dt}+F'(t)\right)}{\tau_{L1}^*\tau_{L2}^*} - \frac{(\tau_{L1}^*+\tau_{L2}^*)\frac{dM'_{ff}(t)}{dt}-M'_{ff}(t)}{\tau_{L1}^*\tau_{L2}^*} \quad \textit{Equation 12}$$

Smith Predictor Derivation

$$G_P^* = \frac{\hat{B}(s)}{MM(s)} = \frac{k_P^* e^{-(\theta_P^* s)}}{\tau_P^* s+1} \quad \textit{Equation 13}$$

$$\hat{B}(s) = \tilde{B}(s)e^{-(\theta_P^* s)} \quad \textit{Equation 14}$$

$$G_P^*(s) = \frac{\tilde{B}'(s)}{MM'(s)} = \frac{k_P^*}{\tau_P^* s+1} \quad \textit{Equation 15}$$

$$\tilde{B}'(s)(\tau_P^* s + 1) = k_P^* MM'(s) \quad \textit{Equation 16}$$

$$\tau_P^*\frac{d\tilde{B}'(t)}{dt} + \tilde{B}'(t) = k_P^* MM'(t) \quad \textit{Equation 17}$$

$$\frac{d\tilde{B}'(t)}{dt} = \frac{k_P^* MM'(t) - \tilde{B}(t)}{\tau_P^*} \quad \textit{Equation 18}$$

$$\tilde{B}(t+\Delta t) = \tilde{B}(t) + \frac{d\tilde{B}(t)}{dt}\Delta t \quad \textit{Equation 19}$$

$$\hat{B}'(\theta) = \tilde{B}'(0) \quad \textit{Equation 20}$$

$$Diff. = BBM - \hat{B} \quad \textit{Equation 21}$$

$$E_1 = \tilde{R} - Diff. \qquad \textit{Equation 22}$$

$$E_2 = E_1 - \tilde{B} \qquad \textit{Equation 23}$$

Ziegler-Nichols Quarter Decay Ratio Response

Table 6. Controller settings based on the Continuous Cycling Method, a strategy developed by Ziegler and Nichols in 1942 *[1]*.

Controller Type	Proportional Gain, Kc	Integral Time, τ_I	Derivative Time, τ_D
Proportional, P	$\frac{1}{K_P^*}\left(\frac{\theta_p^*}{\tau_p^*}\right)^{-1}$	NA	NA
Proportional-integral, PI	$\frac{0.9}{K_P^*}\left(\frac{\theta_p^*}{\tau_p^*}\right)^{-1}$	$3.33(\theta_p^*)$	NA
Proportional-integral-derivative, PID	$\frac{1.2}{K_P^*}\left(\frac{\theta_p^*}{\tau_p^*}\right)^{-1}$	$2.0(\theta_p^*)$	$0.5(\theta_p^*)$